# NATIONAL ADVISORY COMMITTEE FOR AERONAUTICS

**TECHNICAL NOTE 2330**

## WATER-LANDING INVESTIGATION OF A MODEL HAVING HEAVY BEAM LOADINGS AND 0° ANGLE OF DEAD RISE

By A. Ethelda McArver

Langley Aeronautical Laboratory
Langley Field, Va.

Washington
April 1951

NATIONAL ADVISORY COMMITTEE FOR AERONAUTICS

TECHNICAL NOTE 2330

# WATER-LANDING INVESTIGATION OF A MODEL HAVING HEAVY BEAM LOADINGS AND 0° ANGLE OF DEAD RISE

By A. Ethelda McArver

## SUMMARY

A model having heavy beam loadings and an angle of dead rise of 0° was subjected to smooth-water impacts in the Langley impact basin. The tests were made at fixed trims of 6°, 9°, 12°, 15°, 30°, and 45° for a range of flight-path angles from approximately 2° to 22°. Most of the tests were made at a beam-loading coefficient of 18.8, but a few impacts were made at a beam-loading coefficient of 36.5. The data from the higher beam loading were too few, however, to establish quantitatively any effects of variation of beam loading; consequently, trends have been noted only from the data obtained with a beam-loading coefficient of 18.8.

Time histories of horizontal and vertical displacements, vertical velocity, vertical acceleration, and pitching moment were obtained. The results are presented as plots showing the variation of the experimentally determined quantities converted to nondimensional coefficients with flight-path angle at water contact. The impact lift coefficient increases with increasing flight-path angle at water contact, but shows no marked variation with trim angle. The draft coefficients at maximum vertical acceleration and at maximum immersion increase linearly with flight-path angle at water contact and, at maximum vertical acceleration increase with increasing trim; however, at maximum immersion, the draft coefficient is not appreciably affected by trim.

## INTRODUCTION

An experimental program is being conducted at the Langley impact basin to determine the landing-impact characteristics of hydrodynamic configurations having heavy beam loadings. The results of an investigation made on a model having a dead-rise angle of 30° are presented in reference 1. The present investigation was made on a model having a dead-rise angle of 0°, which is one end point of the dead-rise range. Since there are substantial differences between the flow about the

V-bottom configuration of reference 1 and the flow about a flat plate, no direct comparison is made herein of the results of the two investigations.

The test model had a 1-foot beam and was 5 feet long. Most of the impacts were made at a dropping weight of 1176 pounds, corresponding to a beam-loading coefficient of 18.8, and a few runs were made at a dropping weight of 2276 pounds, corresponding to a beam-loading coefficient of 36.5. All landings were made in smooth water.

This paper presents the experimental values of over-all loads and motions and discusses the effects of flight-path angle and trim upon loads obtained with a flat plate.

## SYMBOLS

Physical quantities:

| | |
|---|---|
| $\beta$ | angle of dead rise, degrees |
| $\gamma$ | flight-path angle relative to undisturbed water surface, degrees |
| $\rho$ | density of water (1.938 slugs/cu ft) |
| $\tau$ | trim angle, degrees |
| $b$ | model beam, feet |
| $g$ | acceleration due to gravity (32.2 ft/sec$^2$) |
| $M$ | pitching moment, pound-feet |
| $n_{i_w}$ | impact load factor, measured normal to undisturbed water surface, g units |
| $t$ | time after contact, seconds |
| $V$ | resultant velocity of model, feet per second |
| $W$ | dropping weight, pounds |
| $w$ | specific weight of water (62.4 lb/cu ft) |
| $\dot{x}$ | velocity of model parallel to undisturbed water surface, feet per second |

$y$ immersion of model at step normal to undisturbed water surface, feet

$\dot{y}$ velocity of model normal to undisturbed water surface, feet per second

$c_p$ distance from reference point to center of pressure, feet

Subscripts:

o at water contact

f referred to front fittings

s referred to step (stern of model)

max maximum

Dimensionless variables:

$C_l$ impact lift coefficient $\left(\frac{n i_w W}{\frac{1}{2}\rho V_o^2 b^2}\right)$

$C_d$ draft coefficient $(y/b)$

$C_t$ time coefficient $(V_o t/b)$

$C_m$ pitching-moment coefficient $\left(\frac{M}{\frac{1}{2}\rho V_o^2 b^3}\right)$

$C_{cp}$ center-of-pressure coefficient $(c_p/b)$

$C_\Delta$ beam-loading coefficient $(W/wb^3)$

$\frac{\dot{y}}{\dot{y}_o}$ vertical-velocity ratio

## APPARATUS

The investigation was conducted in the Langley impact basin with the test equipment and instrumentation described in reference 2. The test model was a structural steel channel 5 feet long and 1 foot wide with a

flat bottom machined to a smooth surface. The lines and pertinent dimensions of the model are shown in figure 1.

The model was rigidly attached to a dynamometer which in turn was attached to the carriage boom. Variations in trim were obtained by utilizing various lengths of trim links between the rear attachment point of the dynamometer and boom (fig. 1).

The instrumentation used to measure both the horizontal displacement and velocity and the vertical displacement and velocity was described in reference 2. Accelerations in the vertical direction were measured by two oil-damped unbonded strain-gage-type accelerometers, one having an undamped natural frequency of 105 cycles per second and the other, a natural frequency of 120 cycles per second; both were damped at approximately 65 percent of the critical damping. The initial contact with the water of the model and the rebound of the model from the water were determined by means of an electrical circuit completed by the water. The pitching moments were obtained about the axis a from strain gages mounted on the load-measuring strut as shown in figure 1. Complete time histories of the measured quantities were obtained on a recording oscillograph of which a sample record is presented as figure 2.

## PRECISION

The apparatus used in the present investigation gives measurements that are believed correct within the following limits:

| | |
|---|---|
| Horizontal velocity, feet per second | ±0.5 |
| Vertical velocity at contact, feet per second | ±0.2 |
| Vertical displacement, feet | ±0.03 |
| Acceleration, g | ±0.2 |
| Time, seconds | ±0.005 |
| Weight, pounds | ±2.0 |
| Pitching moment about front fittings, percent | ±5 |

## TEST CONDITIONS

The data used in this investigation were obtained during tests made primarily to obtain information on the distribution of water pressures on the model bottom during landing impacts. Although the number of runs and the combination of independent parameters are somewhat limited, the data are believed sufficient to establish some trends.

The model was tested at 0° yaw and at trims of 6°, 9°, 12°, 15°, 30°, and 45° in smooth water. The majority of the runs were made at a dropping weight of 1176 pounds although three runs using a dropping weight of 2276 pounds were included. The horizontal velocity for these tests ranged from approximately 25 feet per second to 90 feet per second and the vertical velocity ranged from approximately 3 feet per second to 10 feet per second. The depth of immersion of the model was measured in a direction perpendicular to the undisturbed water surface. During the impact process, a lift force equal to the total weight of the model and drop linkage was exerted on the model by means of the lift engine described in reference 2.

## RESULTS AND DISCUSSION

The values of the initial conditions and the recorded data at maximum acceleration, maximum draft, and rebound are presented in table I. The experimentally determined quantities were converted to nondimensional coefficients which have been plotted against flight-path angle at instant of water contact. Since the nondimensional coefficients employed do not include values affected by changes in geometry and loading, the results are valid only for a flat bottom having a constant beam throughout the immersed length and a beam loading corresponding to the test value.

Most of the tests were made at a value of beam-loading coefficient of 18.8. Although a few runs were made at a $C_{\Delta}$ of 36.5, the data at the higher beam loading were too few to determine quantitatively any effects of variation in beam loading.

Figure 3 shows the variation of impact lift coefficient at the instant of maximum acceleration with flight-path angle at the instant of water contact. Inasmuch as the lift engine contributed a force equal to the dropping weight, 1g was subtracted from the values obtained from accelerometer records used in determining $(n_{i_w})_{max}$ in order to isolate the hydrodynamic impact force. Although it was shown in reference 1 that, for a 30° dead rise model and for trims below 30°, a marked variation of impact lift coefficient with trim occurred, this variation is not apparent with the 0° dead rise model. For a beam-loading coefficient of 18.8 the impact lift coefficient at maximum vertical acceleration increases linearly with increasing flight-path angle at water contact but shows no marked variation with trim angle. The test points obtained at a beam-loading coefficient of 36.5 also appear in figure 3; however, lack of an adequate number of test points precludes establishment of any trends.

The variation of draft coefficient at the instant of maximum acceleration with flight-path angle at water contact is shown in figure 4. For a beam-loading coefficient of 18.8 the draft coefficient increases linearly with both increasing flight-path angle and increasing trim, although the points at trims of 9°, 12°, and 15° seem to fall along the same line. Since there is only one point at $C_{\Delta}$ of 36.5 for each trim of 12°, 15° and 30°, it is not possible to interpret the variation of the beam-loading parameter beyond the obvious conclusion that the draft coefficient generally will increase with the beam loading provided the other parameters remain constant.

Figure 5 shows the variation of the draft coefficient at the instant of maximum immersion with flight-path angle at the instant of water contact. For both beam-loading coefficients of 18.8 and 36.5, the draft coefficient increases linearly with flight-path angle at water contact and is not appreciably affected by trim. Here again the test points made at higher values of $C_{\Delta}$ exhibit larger values of $C_d$ than those made at the lower beam loadings.

The vertical-velocity ratios at the instant of maximum acceleration and at the instant of model rebound are plotted against flight-path angle at water contact in figure 6. It is evident from this figure that, for a given initial velocity, the vertical velocity at maximum acceleration increases with initial flight-path angle and decreases with increasing trim angle. For a given initial velocity, however, the upward vertical velocity of rebound decreases with initial flight-path angle and increases with trim. For the lower trims combined with the higher flight-path angles, the vertical-velocity ratios at both maximum acceleration and at model rebound exhibit the least percentage reduction in vertical velocity. The minimum reduction in the vertical velocity at maximum acceleration was less than 20 percent whereas the maximum exceeded 50 percent. At the instant of model rebound the trend is shown to be the same as at maximum acceleration, but in this case the minimum reduction was 130 percent, whereas the maximum was 190 percent.

Figures 7(a), (b), and (c) present the effects of the flight-path angle at water contact upon time to reach maximum acceleration, to reach maximum draft, and for the model rebound, respectively. The time coefficient at the instant of maximum acceleration decreases with increasing flight-path angle and increases as the trim becomes greater. At the instants of maximum immersion and model rebound, the time coefficient, however, increases with increasing flight-path angle and with increasing trim. As would normally be expected, the runs made at a beam-loading coefficient of 36.5 indicate larger time coefficients than those for runs at a lower beam loading.

Figure 8 presents the coefficient of pitching moment about the front fittings at the instant of maximum acceleration as a function of flight-path angle at water contact. Inasmuch as the mass below the dynamometer was an appreciable part of the total mass, corrections were made for the effect of inertia on the recorded pitching-moment data. Since the forces parallel to the bottom are very small, the resultant load is considered normal to the bottom. Hence, the direction of the resultant load is essentially parallel to the center line of the front fittings and the pitching-moment arm can be considered as the distance between the resultant load on the bottom and the center line of the front fittings.

The distance of the center of pressure from the center line of the front fittings is therefore obtained from the relation

$$c_{p_f} = \frac{M_f}{\frac{n_{i_w}}{\cos \tau} W}$$

In order to present the data in a more practical form, the distance of the center of pressure from the center line of the front fittings was subtracted from the distance between the step and front fittings and resulted in values of the distance of the center of pressure $c_{p_s}$ from the step. These values of $c_{p_s}$ obtained at the time of maximum acceleration were divided by model beam to form a nondimensional center-of-pressure coefficient at the time of maximum acceleration and were plotted against flight-path angle at water contact in figure 9. As shown in this figure, at a given flight-path angle the center of pressure moves rearward, as the trim increases. The scatter in the test data can probably be attributed to the fact that two experimentally determined parameters, $n_i$ and $M_f$, with the attendant experimental errors of each, were used in obtaining the location of the center of pressure.

## SUMMARY OF RESULTS

Tests were made in the Langley impact basin to obtain experimental data from smooth-water landing tests of a model having an angle of dead rise of $0^\circ$ and beam-loading coefficients of 18.8 and 36.5. In the tests made at a beam-loading coefficient of 18.8, several flight-path angles were employed for each of six trim angles; whereas, in the tests made

at a beam-loading coefficient of 36.5, only one flight-path angle was employed for each of three trim angles. Since the data from the tests at a beam-loading coefficient of 36.5 were so few, the following conclusions are drawn only for a beam-loading coefficient of 18.8:

1. The impact lift coefficient at maximum vertical acceleration increases linearly with increasing flight-path angle at water contact but shows no marked variation with trim angle.

2. The draft coefficient at maximum acceleration and at maximum immersion increases linearly with flight-path angle at water contact. At maximum vertical acceleration this coefficient generally increases with increasing trim; whereas, at maximum immersion it is not appreciably affected by trim.

3. For a given initial velocity, the vertical velocity at maximum acceleration increases with initial flight-path angle and decreases with trim angle; however, the upward velocity of rebound decreases with initial flight-path angle and increases with trim.

4. The time coefficient at maximum vertical acceleration decreases with increasing flight-path angle at water contact and increases with increasing trim angle; whereas, for the time coefficients at maximum draft and at model rebound, the reverse is true.

5. The center-of-pressure coefficient at maximum vertical acceleration referred to the step increases with increasing flight-path angle at water contact and decreases with increasing trim angle.

Langley Aeronautical Laboratory
National Advisory Committee for Aeronautics
Langley Field, Va., January 17, 1951

## REFERENCES

1. Batterson, Sidney A., and McArver, A. Ethelda: Water Loading Investigation of a Model Having a Heavy Beam Loading and a 30° Angle of Dead Rise. NACA TN 2015, 1950.

2. Batterson, Sidney A.: The NACA Impact Basin and Water Landing Tests of a Float Model at Various Velocities and Weights. NACA Rep. 795, 1944.

TABLE I

DATA FROM TESTS OF A MODEL HAVING HEAVY BEAM LOADINGS AND 0° ANGLE OF DEAD RISE

| Run | $\tau$ (deg) | At contact | | | | At $(n_{i_w})_{max}$ | | | | | At $y_{max}$ | | At rebound | |
|---|---|---|---|---|---|---|---|---|---|---|---|---|---|---|
| | | $V_o$ (fps) | $\dot{y}_o$ (fps) | $\dot{x}_o$ (fps) | $\gamma_o$ (deg) | t (sec) | $n_{i_w}$ (g) | y (ft) | $\dot{y}$ (fps) | $M_f$ (lb-ft) | t (sec) | y (ft) | t (sec) | $\dot{y}$ (fps) |
| W = 1176 lb; $C_\Delta$ = 18.8 | | | | | | | | | | | | | | |
| 1 | 6 | 80.1 | 2.9 | 80.0 | 2.06 | 0.052 | 0.9 | 0.12 | 1.9 | 2,009 | 0.140 | 0.18 | 0.273 | -1.2 |
| 2 | | 51.9 | 2.6 | 51.9 | 2.85 | .060 | .6 | .15 | 1.9 | 983 | .205 | .26 | .469 | -1.0 |
| 3 | | 44.8 | 2.6 | 44.7 | 3.30 | .070 | .5 | .17 | 1.9 | 741 | .230 | .30 | .562 | -.9 |
| 4 | | 44.2 | 5.8 | 43.8 | 7.58 | .046 | 1.1 | .26 | 5.0 | 1,256 | .315 | .71 | .811 | -1.8 |
| 5 | 9 | 86.4 | 2.7 | 86.4 | 1.79 | .051 | 1.1 | .12 | 1.6 | 3,116 | .104 | .15 | .200 | -1.9 |
| 6 | | 85.9 | 5.2 | 85.7 | 3.46 | .048 | 1.8 | .23 | 3.6 | 3,659 | .123 | .32 | .260 | -3.0 |
| 7 | | 86.2 | 5.3 | 86.0 | 3.49 | .046 | 1.8 | .21 | 3.8 | 4,037 | .124 | .32 | .253 | -3.0 |
| 8 | | 44.0 | 3.8 | 44.0 | 4.96 | .071 | .7 | .24 | 2.8 | 1,045 | .217 | .39 | .541 | -1.6 |
| 9 | | 44.7 | 4.6 | 44.4 | 5.86 | .071 | .8 | .31 | 3.5 | 1,324 | .246 | .53 | .598 | -1.9 |
| 10 | 12 | 62.7 | 5.2 | 62.5 | 4.75 | .058 | 1.3 | .28 | 3.7 | 2,902 | .159 | .44 | .338 | -3.0 |
| 11 | | 61.8 | 5.4 | 61.5 | 4.97 | .058 | 1.3 | .26 | 3.8 | 3,003 | .163 | .40 | .341 | -2.9 |
| 12 | | 40.5 | 4.7 | 40.2 | 6.69 | .077 | .9 | .34 | 3.5 | 1,311 | .247 | .55 | .583 | -2.1 |
| 13 | | 44.4 | 7.6 | 43.8 | 9.89 | .052 | 1.4 | .38 | 6.3 | 2,255 | .237 | .83 | .599 | -2.9 |
| 14 | 15 | 86.1 | 4.1 | 86.0 | 2.72 | .059 | 2.0 | .22 | 2.1 | 5,027 | .097 | .23 | .195 | -3.4 |
| 15 | | 62.7 | 4.9 | 62.5 | 4.51 | .068 | 1.4 | .28 | 2.9 | 3,111 | .148 | .36 | .296 | -3.1 |
| 16 | | 39.6 | 4.1 | 39.3 | 5.99 | .084 | .7 | .31 | 3.0 | 1,301 | .220 | .51 | .540 | -2.0 |
| 17 | | 44.2 | 7.7 | 43.5 | 10.05 | .064 | 1.5 | .44 | 5.9 | 2,446 | .234 | .82 | .546 | -3.3 |
| 18 | 30 | 62.3 | 3.2 | 62.2 | 2.97 | .084 | 1.2 | .18 | 1.5 | 3,694 | .131 | .21 | .238 | -2.8 |
| 19 | | 62.8 | 6.4 | 62.5 | 5.81 | .078 | 1.9 | .38 | 3.7 | 5,356 | .145 | .47 | .291 | -4.8 |
| 20 | | 39.7 | 6.8 | 39.1 | 9.92 | .092 | 1.3 | .54 | 4.9 | 2,548 | .236 | .81 | .508 | -4.2 |
| 21 | | 25.2 | 9.1 | 23.5 | 21.21 | .125 | 1.0 | 1.01 | 6.6 | 1,506 | .388 | 1.68 | 1.033 | -3.2 |
| 22 | 45 | 39.9 | 6.9 | 39.3 | 9.95 | .164 | 1.3 | .86 | 2.9 | ----- | .248 | .92 | .516 | -4.8 |
| 23 | | 26.7 | 9.3 | 25.0 | 20.36 | .178 | .9 | 1.33 | 5.7 | ----- | .391 | 1.78 | .958 | -3.9 |
| W = 2276 lb; $C_\Delta$ = 36.5 | | | | | | | | | | | | | | |
| 24 | 12 | 41.0 | 5.1 | 40.7 | 7.13 | 0.135 | 0.5 | 0.56 | 3.5 | ----- | 0.400 | 0.86 | 0.984 | -1.4 |
| 25 | 15 | 36.8 | 5.2 | 36.4 | 8.11 | .142 | .6 | .61 | 3.4 | ----- | .410 | 1.00 | 1.093 | -1.5 |
| 26 | 30 | 41.3 | 7.2 | 40.7 | 10.05 | .142 | 1.0 | .93 | 4.8 | ----- | .334 | 1.30 | .756 | -4.2 |

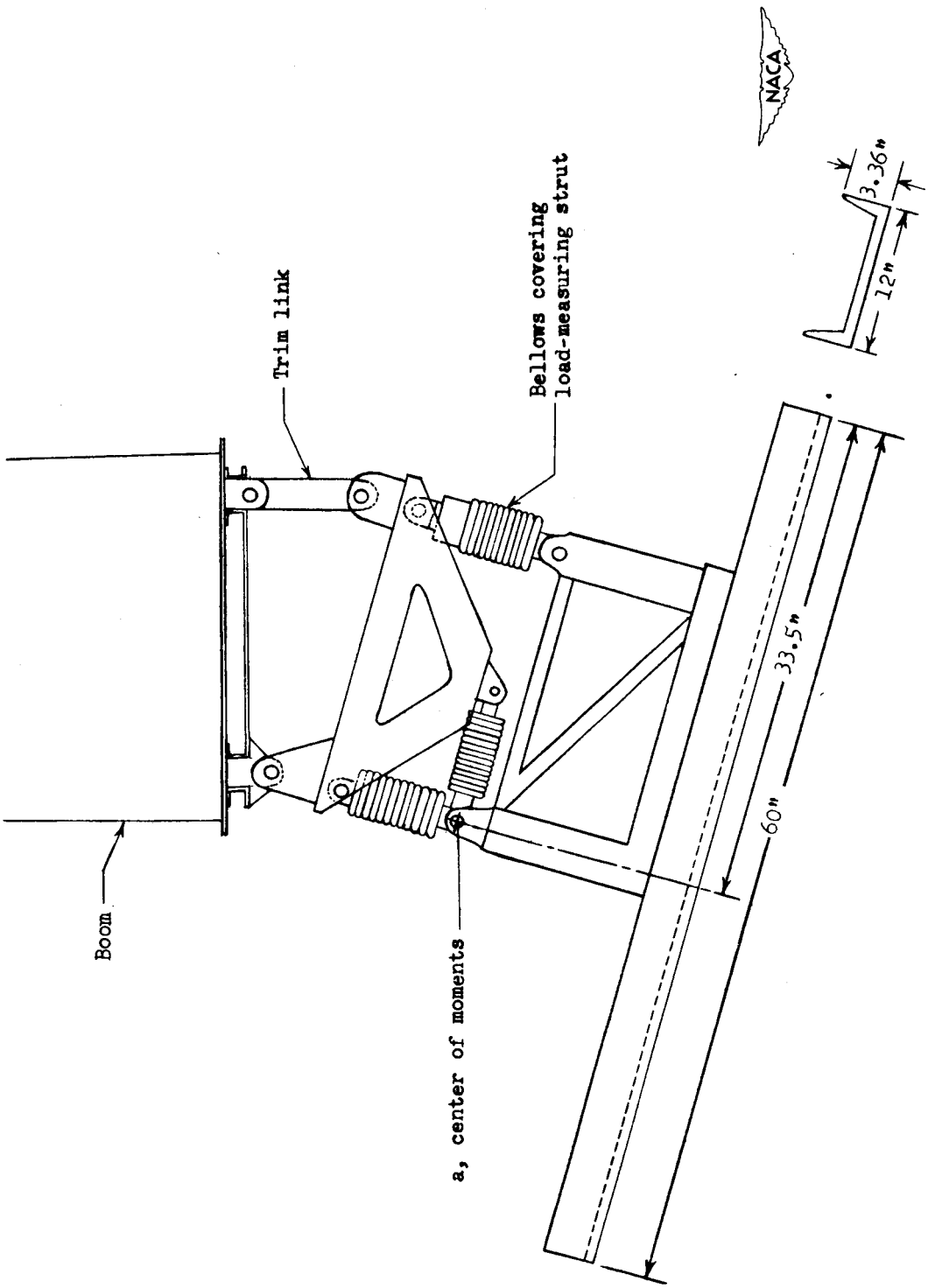


Figure 1.- Lines and pertinent dimensions of model tested in Langley impact basin.

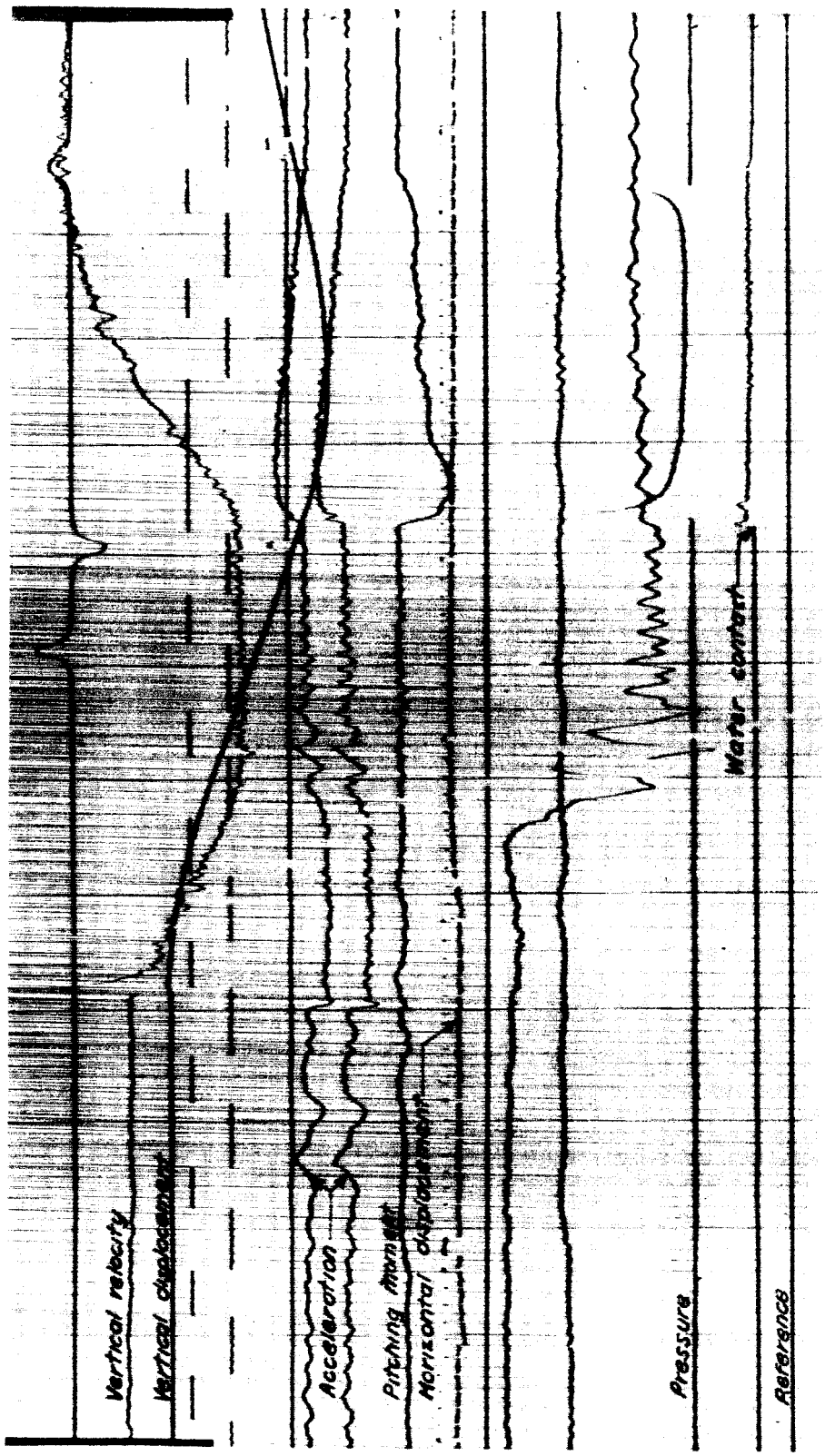


Figure 2.- Oscillograph record obtained during run 10 at the Langley impact basin. $\dot{x}_o = 62.5$; $\dot{y}_o = 5.19$.

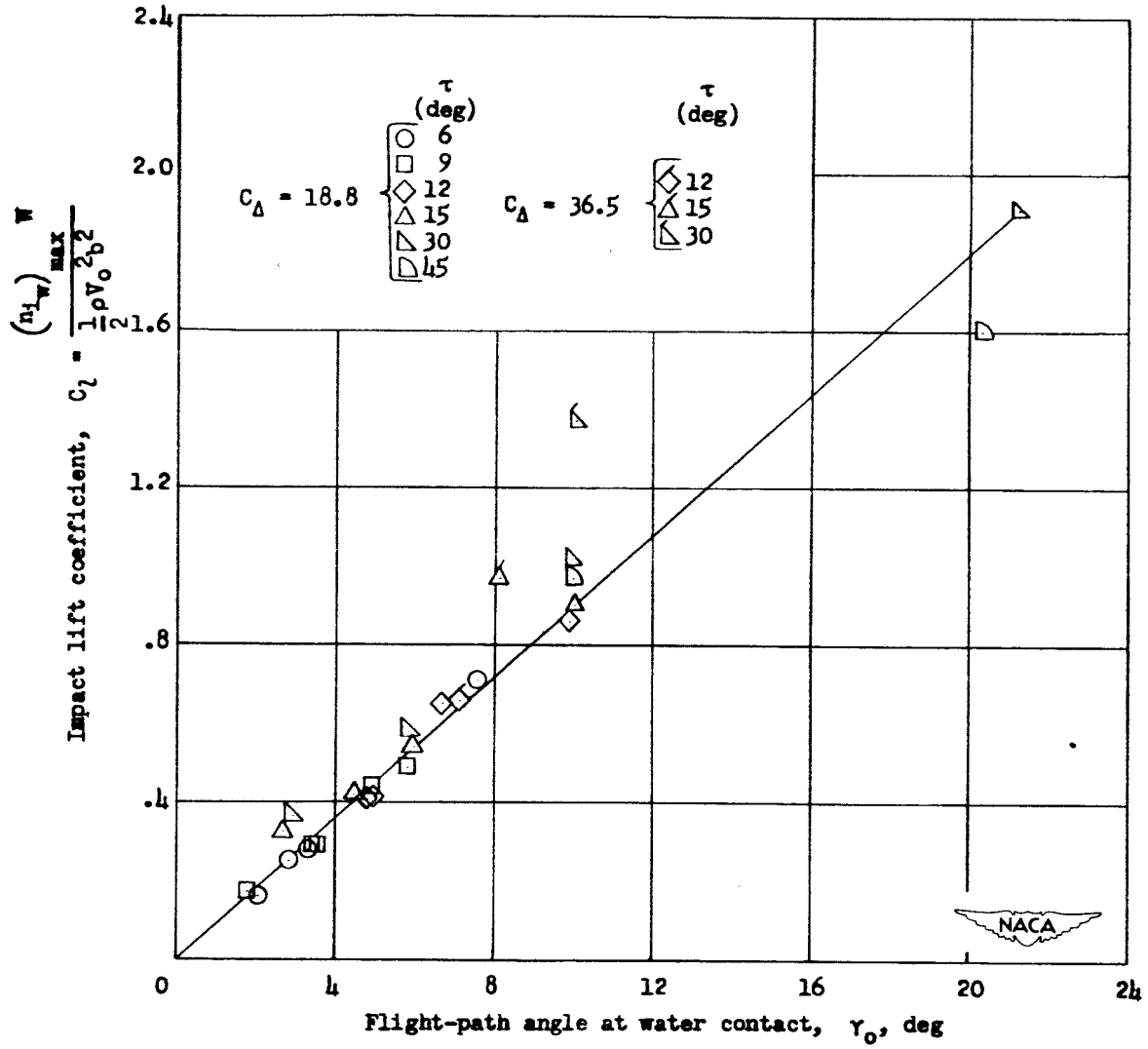


Figure 3.- Variation of impact lift coefficient at instant of maximum acceleration with flight-path angle at water contact. $\beta = 0^\circ$.

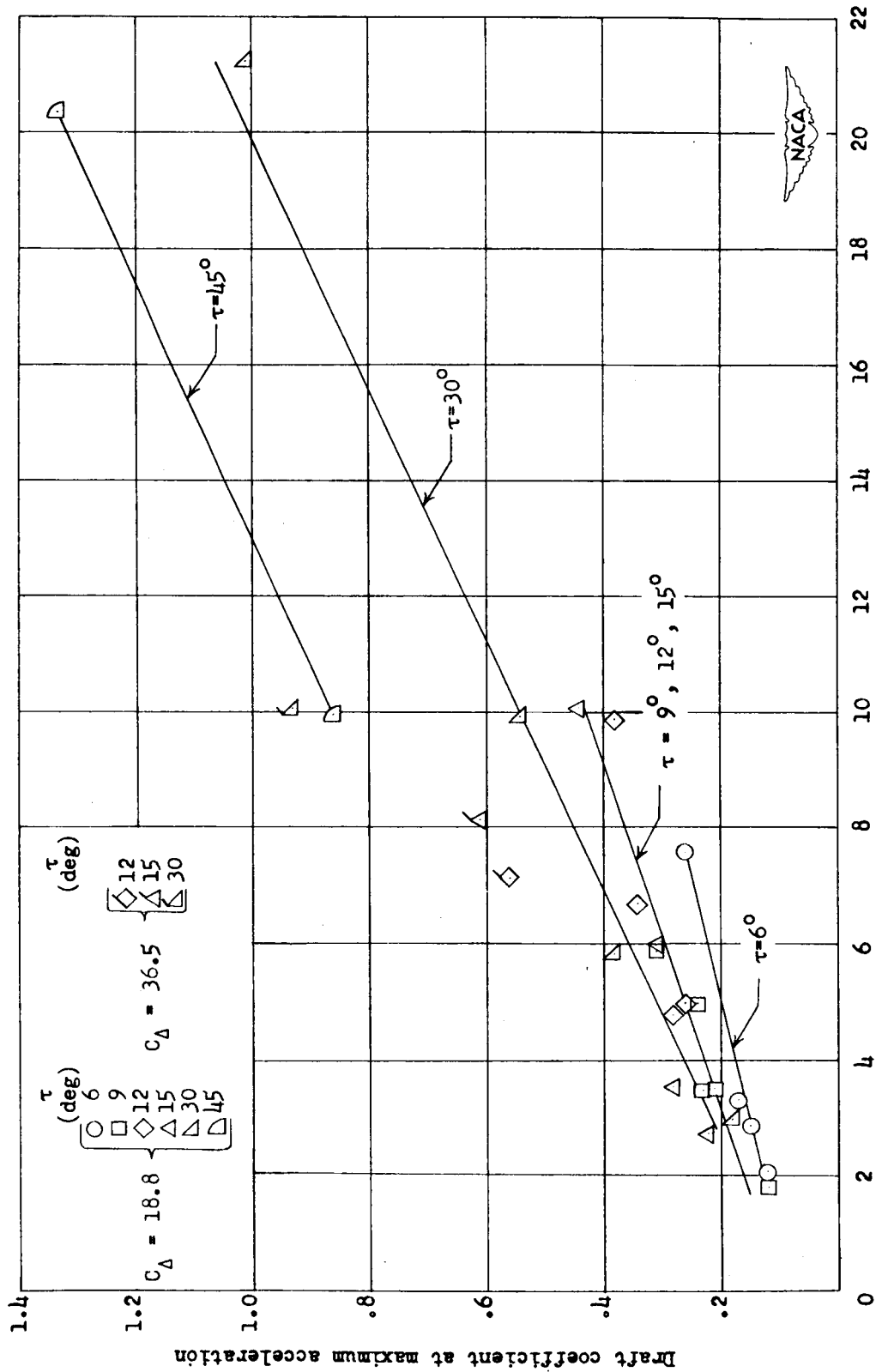


Figure 4.- Variation of draft coefficient at the instant of maximum acceleration with flight-path angle at water contact. $\beta = 0°$.

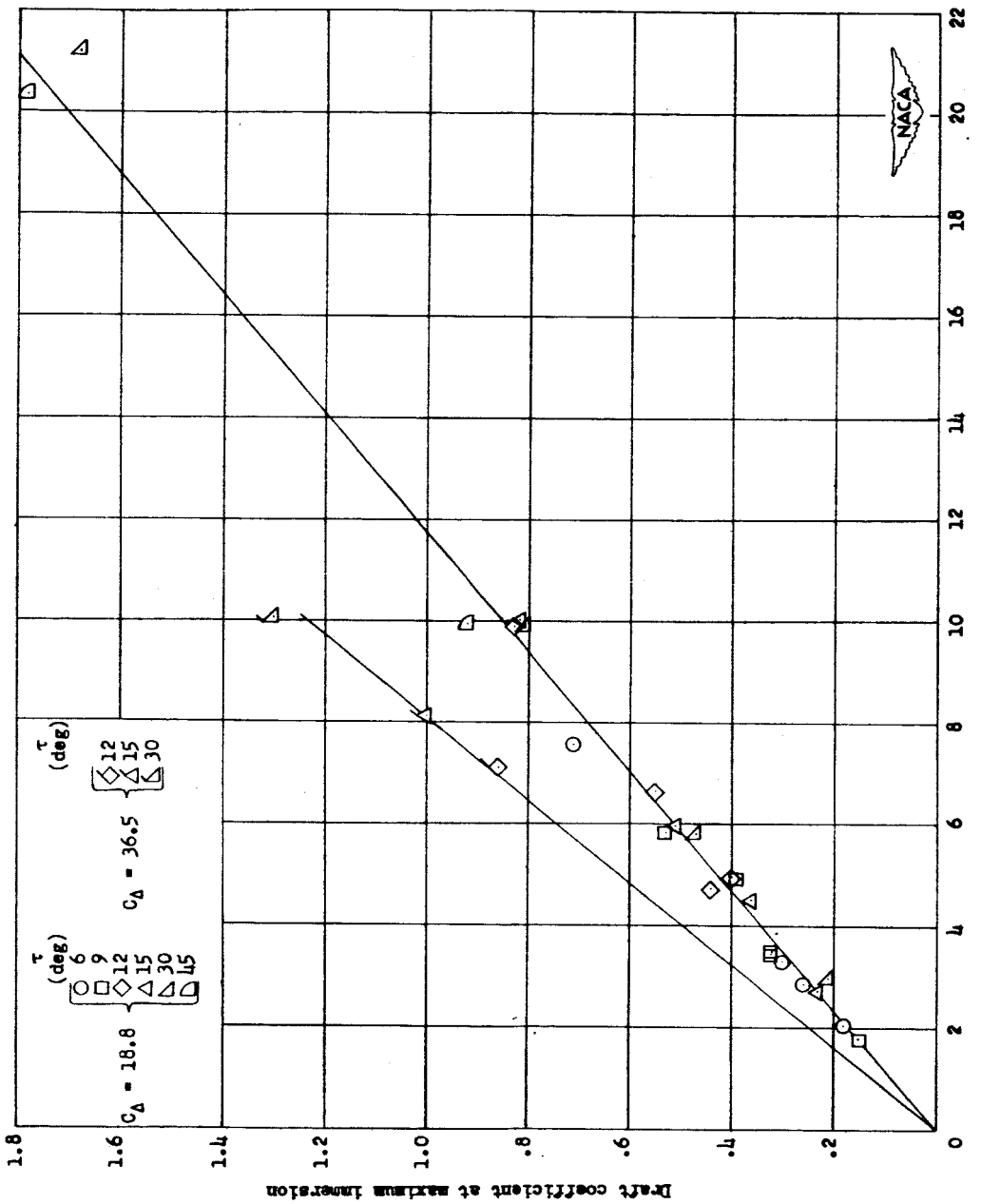


Figure 5.- Variation of draft coefficient at the instant of maximum immersion with flight-path angle at water contact. $\beta = 0^\circ$.

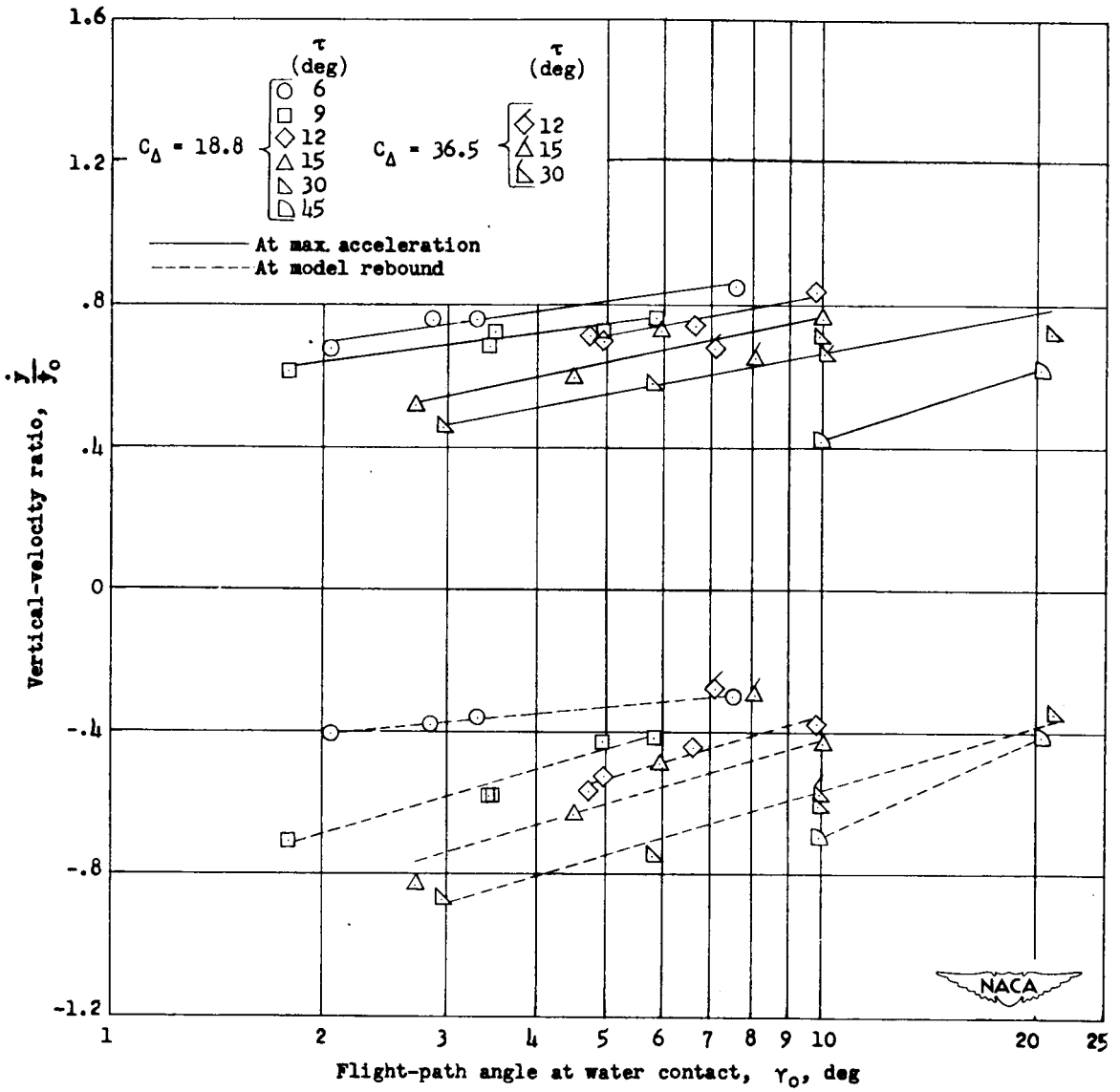


Figure 6.- Variation of vertical-velocity ratio with flight-path angle at water contact. $\beta = 0^\circ$.

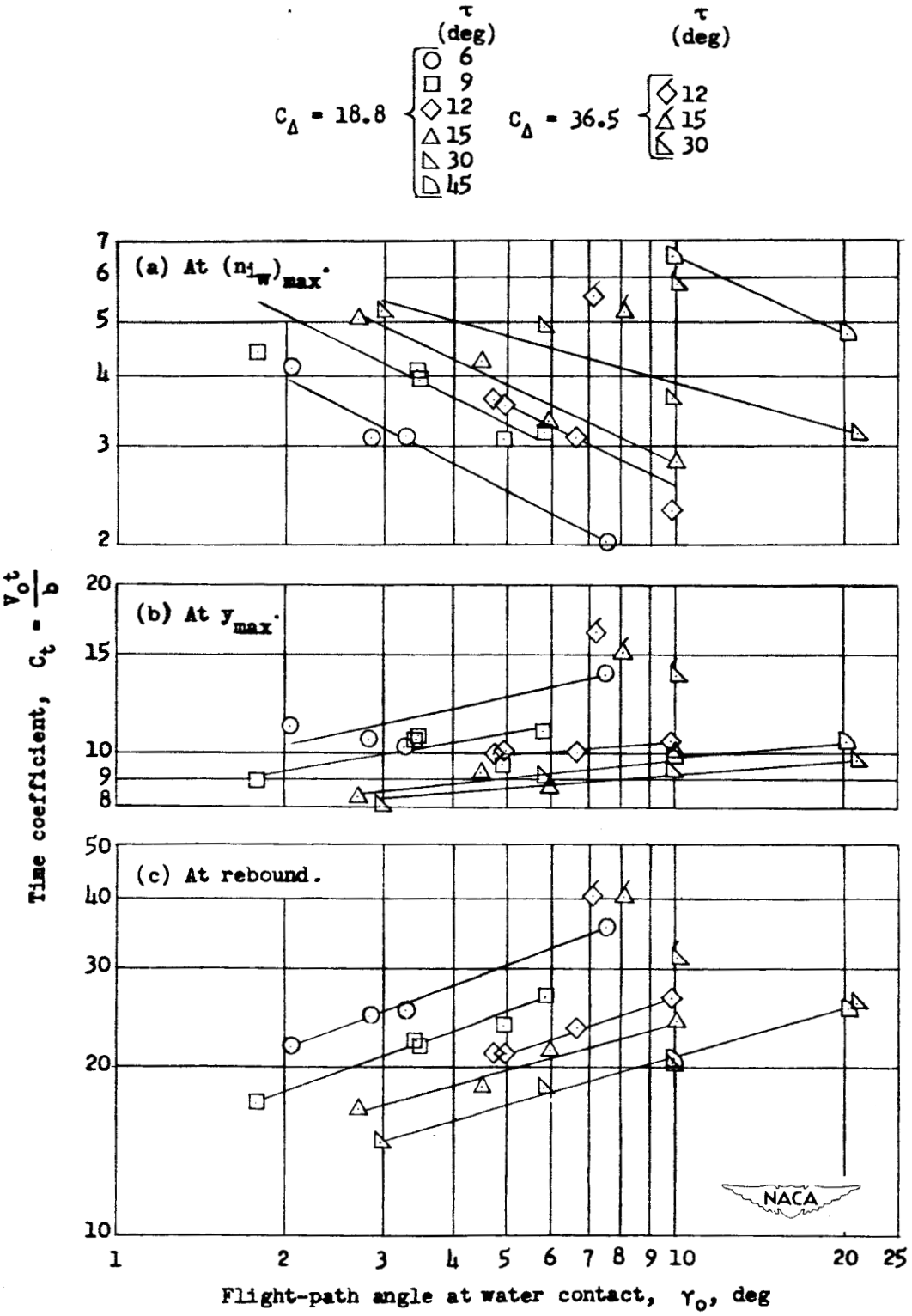


Figure 7.- Variation of time coefficient with flight-path angle at water contact. $\beta = 0^\circ$.

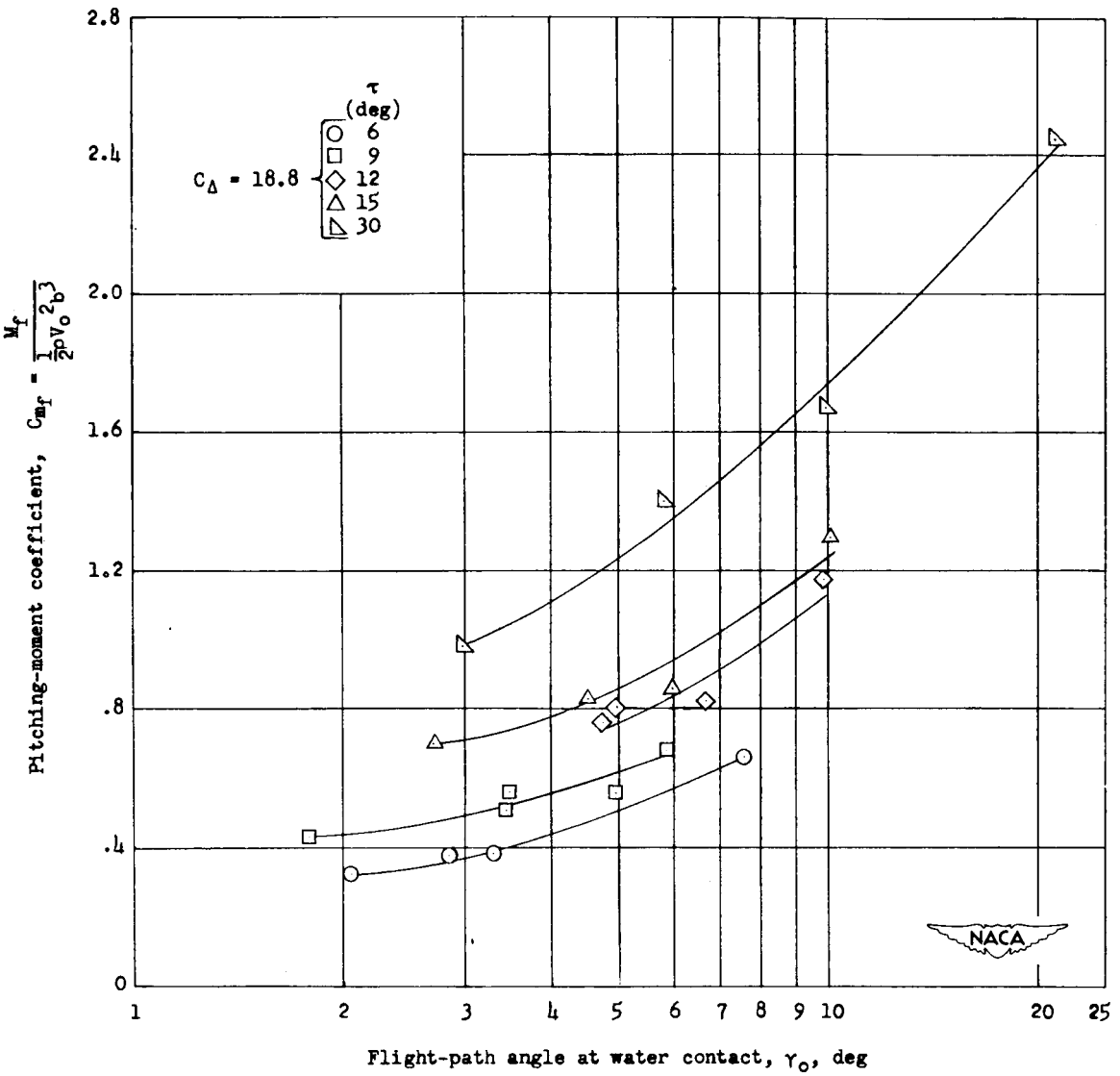


Figure 8.- Variation of pitching-moment coefficient about the front fittings at the instant of maximum acceleration with flight-path angle at water contact. $\beta = 0^\circ$.

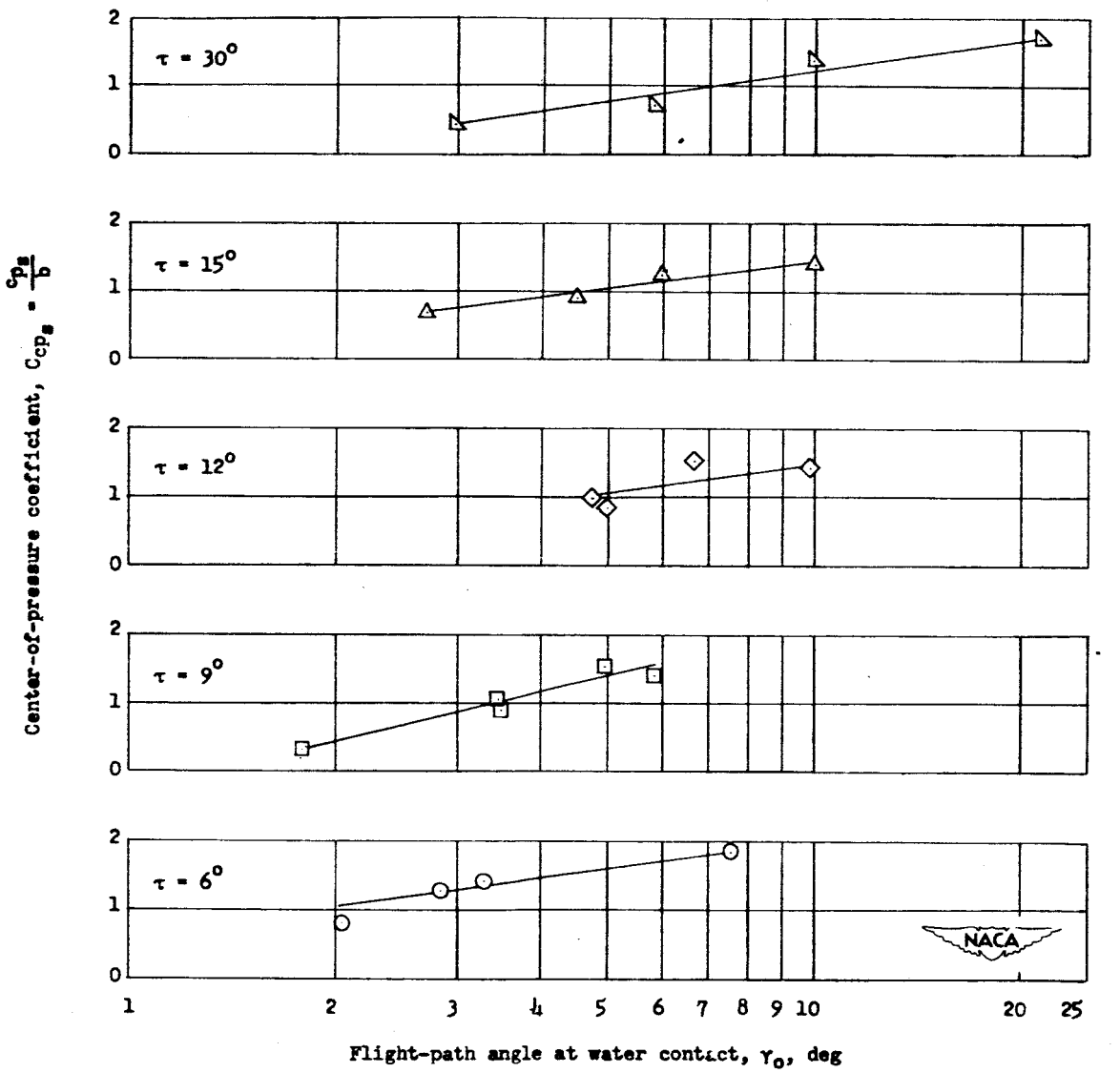


Figure 9.- Variation of center-of-pressure coefficient at maximum acceleration referred to step with flight-path angle at water contact. $\beta = 0^\circ$; $C_\Delta = 18.8$.